Experimental and Monte Carlo Investigation of Intrinsic Limits of Scintillator Energy Resolution

Bryan W. Reutter, *Senior Member, IEEE,* William W. Moses, *Fellow, IEEE,* Woon-Seng Choong, *Member, IEEE,* Giulia Hull, Stephen A. Payne, Nerine J. Cherepy, and John D. Valentine, *Senior Member, IEEE*

***Abstract*—While non-proportionality is assumed to degrade scintillator energy resolution, the quantitative relationship between non-proportionality and energy resolution is not well understood. We report on the results of experimental data analysis and Monte Carlo simulation used jointly to study the relationship between scintillator electron response non-proportionality and gamma ray energy resolution. Energy resolution for Compton interactions was compared to energy resolution for photoelectric interactions, to investigate the hypothesis that non-proportionality affects these two types of interactions differently. The difference is thought to be due to low energy quanta such as Auger electrons and fluorescent x-rays produced by photoelectric interactions (which predominantly interact with inner shell electrons) but not by Compton interactions (which predominantly interact with valence electrons). A newly constructed Compton coincidence apparatus (SLYNCI) was used to measure electron response non-proportionality in NaI(Tl) that was excited by Compton-scattered electrons. Measured values for both light output vs. electron energy and energy resolution vs. electron energy were then used to predict gamma ray energy resolution, based on Monte Carlo simulations that mimicked the distribution of energetic electrons emitted following photoelectric absorption of gamma rays in the scintillator. Predicted values were compared to experimental data obtained by exciting the scintillator with isotopic sources. In this manner, the component of gamma ray energy resolution degradation due to non-proportionality was determined, as well as the electron energy resolution component due to electron response counting statistics and other possible limiting factors such as Landau fluctuations in the dE/dx along the electron track.**

***Index Terms*—Scintillator non-proportionality, energy resolution, Compton coincidence technique**

I. Introduction

THE OVERARCHING goals of this work are (1) to quantitatively understand the relationship between non-proportionality and energy resolution, (2) to understand differences in energy resolution predicted by counting statistics and observed for electron excitation and gamma ray excitation (*e.g.*, Fig. 1), and (3) to compare measured gamma ray energy resolution to predictions obtained from measured electron response and models for photon transport and electron cascade mechanisms.

This work was supported by the National Nuclear Security Administration, Office of Defense Nuclear Nonproliferation, Office of Nonproliferation Research and Development (NA-22) of the U. S. Department of Energy under Contract No. DE-AC03-76SF00098.

B. W. Reutter, W. W. Moses, and W.-S. Choong are with Lawrence Berkeley National Laboratory, One Cyclotron Road, Berkeley, CA 94720 USA (e-mail: bwreutter@lbl.gov).

G. Hull, S. A. Payne, N. J. Cherepy, and J. D. Valentine are with Lawrence Livermore National Laboratory, 7000 East Avenue, Livermore, CA 94550 USA.

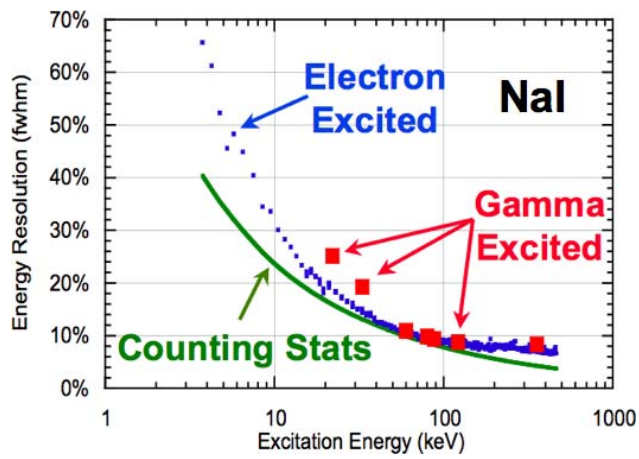

Fig. 1. Comparison of energy resolution of NaI(Tl) predicted by counting statistics and observed for electron excitation and gamma ray excitation.

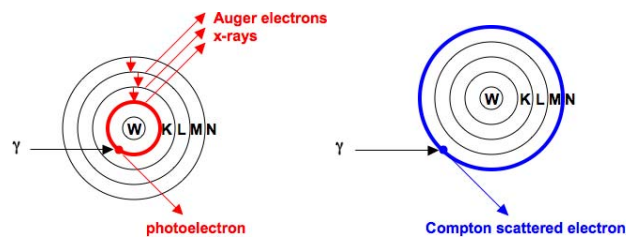

Fig. 2. (Left) Photoelectric interactions usually occur with inner shell electrons, leading to low-energy Auger electrons and fluorescent x-rays. (Right) Compton interactions usually occur with outer shell electrons, which do not produce these low-energy quanta

It has been hypothesized that non-proportionality affects photoelectric interactions very differently than Compton interactions [1], [2]. Photoelectric interactions usually occur with inner shell electrons, leading to low-energy Auger electrons and fluorescent x-rays (Fig. 2, left). Compton interactions usually occur with outer shell electrons, which do not produce these low-energy quanta (Fig. 2, right).

To investigate this hypothesis, we performed experiments in which an NaI(Tl) scintillator was excited by isotopic sources to measure photoelectric interactions, and also by a newly constructed Compton coincidence apparatus known as SLYNCI (Scintillator Light Yield Non-Proportionality Characterization Instrument [3]) to measure Compton interactions. The electron light output and energy resolution measured by SLYNCI were then used as inputs to Monte Carlo simulations that mimicked the cascade of energetic electrons emitted following photo-

electric absorption of gamma rays and yielded predictions of gamma energy resolution.

This work builds on previous research in which gamma ray light output and the non-proportionality component of gamma ray energy resolution are calculated from measured electron light output [4], [5]. In particular, we incorporate experimental measurements of the electron energy resolution component along with the non-proportionality component to predict gamma ray energy resolution for isotopic sources.

II. Methods

A. Measurement of Electron Response and Energy Resolution

Fig. 3 depicts SLYNCI, a newly constructed, high throughput, Compton coincidence apparatus [3]. SLYNCI can measure a scintillator sample in just one day, compared to the month that it took for an earlier instrument [6]. Energetic electrons are produced from Compton scattered gamma rays within the scintillator. The scattered electron absorbed in the scintillator is detected in coincidence with the scattered photon in an HPGe detector. The electron energy is calculated as the difference between the source energy and the energy of the photon detected by the HPGe detector. Electron response is measured at various energies by varying the angle between the gamma source and an array of five HPGe detectors.

SLYNCI data also contain coincident events in which the Compton scattered photon undergoes additional scatter in an HPGe detector (Fig. 4). These events are trimmed and Gaussians are fitted to vertical profiles through the data (Fig. 5) to measure the expected value of the electron light output (location of the peak) and the electron energy resolution (width of the peak). The measured electron energy resolution contains components due to electron response counting statistics, as well as other possible intrinsic limiting factors such as Landau fluctuations in the dE/dx along the electron track.

B. Prediction of Gamma Ray Energy Resolution

Given SLYNCI-measured electron response and energy resolution as input data, we use models for photon transport and simplified electron cascade mechanisms (Fig. 6) in Monte Carlo software simulations to predict gamma ray energy resolution.

With use of the GEANT4 software package [7], each incident photon is tracked through Compton interactions (if any) until it is photoelectrically absorbed. A cascade of quanta is then randomly selected from the cascades depicted in Fig. 6. Fluorescent x-rays generated by iodine K-shell interactions are assumed to be absorbed immediately via photoelectric interactions with the L- or M-shells. Therefore, the net result for each simulated incident photon is a random collection of energetic Compton-scattered electrons (if any), photoelectrons, and Auger electrons.

1) Statistical Modeling: The total light output, L_γ, associated with an incident photon with energy E_γ is modeled to be the sum of the light outputs from the energetic electrons:

$$L_\gamma = \sum_{q=1}^{N_q} L_q, \tag{1}$$

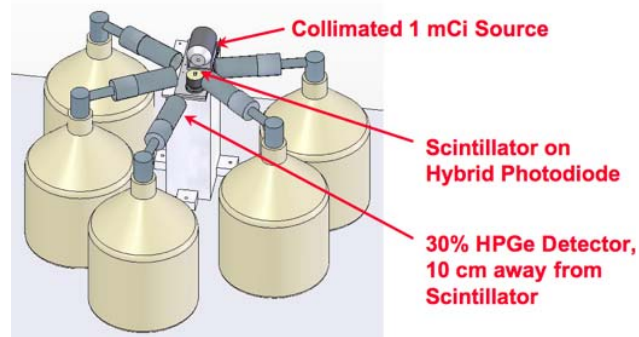

Fig. 3. Depiction of SLYNCI, a newly constructed, high throughput, Compton coincidence apparatus [3].

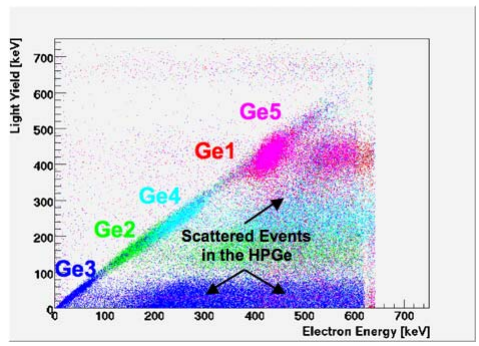

Fig. 4. Data from five HPGe detectors also contain events in which Compton scattered photons undergo additional scatter in the HPGe detectors.

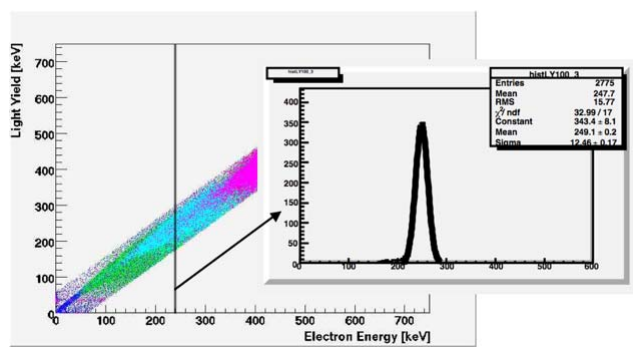

Fig. 5. Scattered events in the HPGe detectors are trimmed and Gaussians are fitted to vertical profiles through the data. The location and width of the peak provide estimates of the expected value of the electron light output and electron energy resolution, respectively.

where L_q are the light outputs from the energetic electrons and there are at most N_q electrons. The expected value of the total light output, given the energies E_q of the electrons, is calculated from measured peak locations in the SLYNCI data (Fig. 5):

$$\mathsf{E}(L_\gamma|\mathbf{E}) = \sum_{q=1}^{N_q} \mathsf{E}(L_q|E_q), \tag{2}$$

where $\mathbf{E} = [E_1 \cdots E_{N_q}]$, $\sum_{q=1}^{N_q} E_q = E_\gamma$ (*i.e.*, energy is conserved), and $\mathsf{E}(\cdot)$ is the expectation operator. The overall average value of the total light output is obtained by averaging

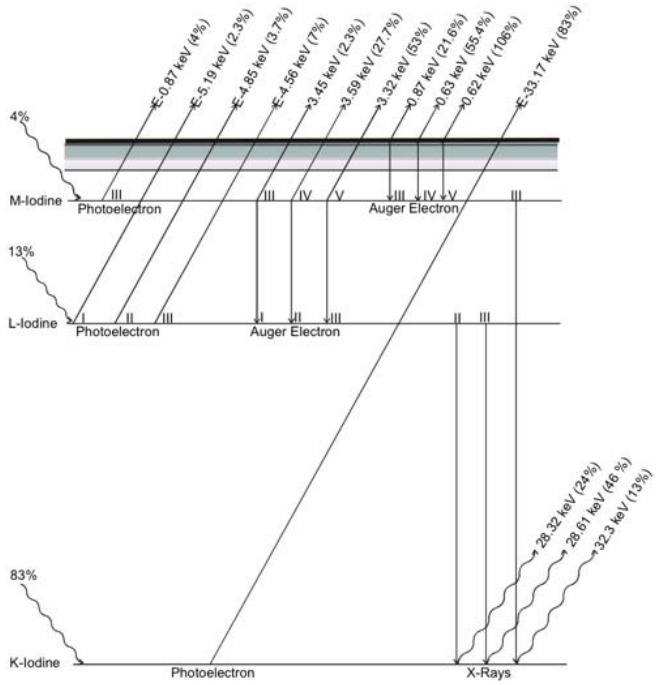

Fig. 6. Model for electron cascade sequences in NaI(Tl) taken from [4]. E denotes the photoelectrically absorbed photon energy.

over light outputs associated with all possible collections of electron energies:

$$\mathsf{E}(L_\gamma) = \mathsf{E}\big[\mathsf{E}(L_\gamma|\mathbf{E})\big] = \int_{\mathcal{D}} \mathsf{Pr}(\mathbf{E}) \sum_{q=1}^{N_q} \mathsf{E}(L_q|E_q) d\mathbf{E}, \quad (3)$$

where $\mathsf{Pr}(\mathbf{E})$ is the probability distribution for the collection of electron energies and $\mathcal{D}$ is the domain of electron energies over which $E_q \geq 0$ and $\sum_{q=1}^{N_q} E_q = E_\gamma$.

Similarly, the variance of the total light output, given the energies E_q of the electrons, is calculated from the variances of Gaussians that are fitted to vertical profiles through the SLYNCI data (Fig. 5):

$$\mathsf{var}(L_\gamma|\mathbf{E}) = \sum_{q=1}^{N_q} \mathsf{var}(L_q|E_q), \quad (4)$$

where it is assumed that fluctuations in the L_q are statistically independent. Taking into account all possible collections of electron energies, the overall variance is given by the law of total variance [8]:

$$\mathsf{var}(L_\gamma) = \mathsf{E}\big[\mathsf{var}(L_\gamma|\mathbf{E})\big] + \mathsf{var}\big[\mathsf{E}(L_\gamma|\mathbf{E})\big], \quad (5)$$

where

$$\mathsf{E}\big[\mathsf{var}(L_\gamma|\mathbf{E})\big] = \int_{\mathcal{D}} \mathsf{Pr}(\mathbf{E}) \mathsf{var}(L_\gamma|\mathbf{E}) d\mathbf{E} \quad (6)$$

$$\mathsf{var}\big[\mathsf{E}(L_\gamma|\mathbf{E})\big] = \int_{\mathcal{D}} \mathsf{Pr}(\mathbf{E}) \big[\mathsf{E}(L_\gamma|\mathbf{E}) - \mathsf{E}(L_\gamma)\big]^2 d\mathbf{E}. \quad (7)$$

Eqn. (6) gives the component of gamma light output variance that is due to the average variance of electron light output, while (7) gives the component of gamma light output variance due to non-proportionality. For an ideal scintillator with proportional light output, $\mathsf{E}(L_\gamma|\mathbf{E})$ is identically equal to $\mathsf{E}(L_\gamma)$ for all collections of electron energies $\mathbf{E}$, and the non-proportionality component of gamma light output variance given by (7) is zero.

2) Analytic Expressions for Discretely-Distributed Electron Energy: For collections of electrons with discretely-valued energy, such as depicted in Fig. 6, the probability distribution for the electron energies can be written as

$$\mathsf{Pr}(\mathbf{E}) = \sum_{c=1}^{N_c} \mathsf{Pr}(\mathbf{E} = \mathbf{E}^c) \delta(\mathbf{E} - \mathbf{E}^c), \quad (8)$$

where $\mathbf{E}^c = [E_1^c \cdots E_{N_q}^c]$ denotes the (known) energies of the electrons in collection c, $\sum_{q=1}^{N_q} E_q^c = E_\gamma$, N_c is the number of possible collections, and $\delta(\cdot)$ denotes the Dirac delta function. Substituting (8) into (3) yields an expression for the expected value of the gamma ray light output:

$$\mathsf{E}(L_\gamma) = \sum_{c=1}^{N_c} \mathsf{Pr}(\mathbf{E} = \mathbf{E}^c) \sum_{q=1}^{N_q} \mathsf{E}(L_q|E_q = E_q^c). \quad (9)$$

Similarly, substituting (8), (4), and (2) into (6) and (7), and then substituting (6) and (7) into (5), yields an expression for the variance of the gamma ray light output:

$$\mathsf{var}(L_\gamma) = \sum_{c=1}^{N_c} \mathsf{Pr}(\mathbf{E} = \mathbf{E}^c) \left\{ \left(\sum_{q=1}^{N_q} \mathsf{var}(L_q|E_q = E_q^c) \right) + \left[\left(\sum_{q=1}^{N_q} \mathsf{E}(L_q|E_q = E_q^c) \right) - \mathsf{E}(L_\gamma) \right]^2 \right\}. \quad (10)$$

3) Monte Carlo Sampling of Continuously-Distributed Electron Energy: The Monte Carlo software simulations provide samples of the probability distribution for collections of electrons that may contain Compton scattered electrons with continuously-valued energy. Given SLYNCI-measured electron response and energy resolution, as well as the outcome of N_c Monte Carlo realizations (*i.e.*, N_c random collections of electrons with energies $\mathbf{E}^c$), (9) and (10) are used with $\mathsf{Pr}(\mathbf{E} = \mathbf{E}^c) = 1/N_c$ to estimate the expected value and variance of gamma ray light output, respectively.

III. Results

A. SLYNCI Measurements Extrapolated to Low Energy

Values for electron light output and energy resolution measured by SLYNCI are shown as circles in Figs. 7 and 8. Prediction of gamma energy resolution from these data requires that the values be extrapolated to zero energy.

Fig. 7 shows three different extrapolations of electron relative light output (*i.e.*, the expected light output per unit energy, $\mathsf{E}(L_q|E_q)/E_q$, normalized to unity at a convenient energy). The extrapolations flatten out at low energies at relative values of 1.0, 0.9, and 0.8, respectively.

Fig. 8 shows two different extrapolations of electron energy resolution, which were obtained by fitting and extrapolating

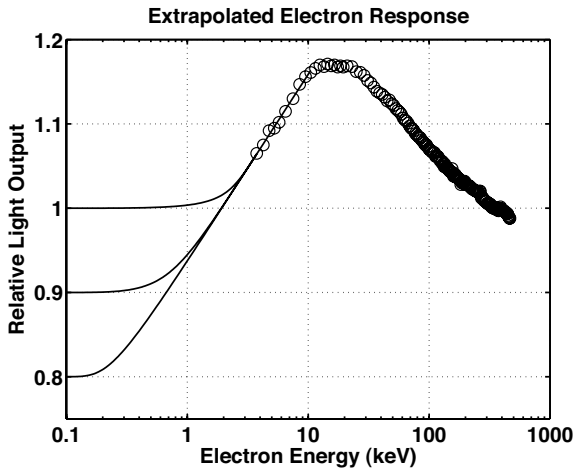

Fig. 7. Circles depict SLYNCI measurements of expected value of electron relative light output (*i.e.*, locations of peaks in Fig. 5). Three different low energy extrapolations are shown.

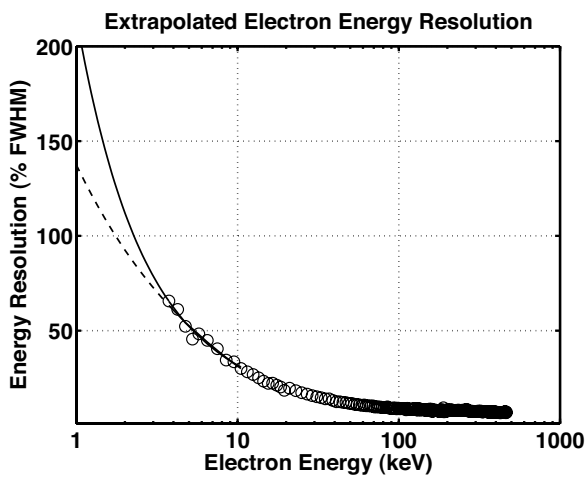

Fig. 8. Circles depict SLYNCI measurements of electron energy resolution (*i.e.*, widths of peaks in Fig. 5). Two different low energy extrapolations are shown. Solid and dashed lines correspond to noise models 1 and 2, respectively, shown in Fig. 9.

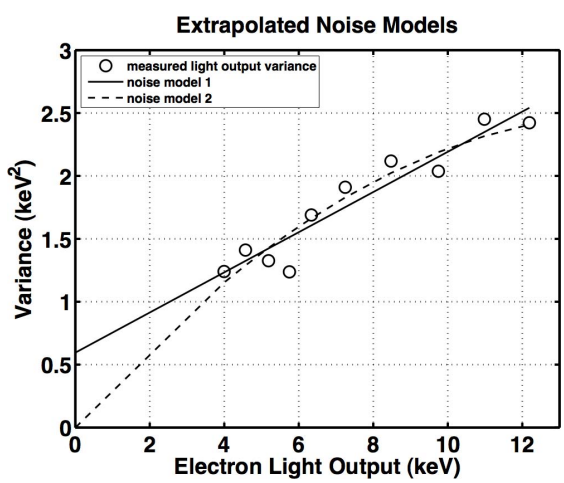

Fig. 9. Solid and dashed lines show fits of noise models 1 and 2, respectively, to SLYNCI measurements of variance of electron light output, depicted by circles. Noise model 1 is linear, and noise model 2 is quadratic and passes through zero.

two different noise models to the measured variance in light output (Fig. 9). The linear extrapolation (noise model 1) yields an energy resolution of about 210% at 1 keV, while the quadratic extrapolation that passes through zero (noise model 2) yields an energy resolution of about 140% at 1 keV.

B. Measured and Predicted Gamma Ray Energy Resolution

Fig. 10 shows reasonable agreement between measured and predicted gamma energy resolution, and that the predicted gamma energy resolution depends primarily on which noise model is used. Fig. 11 shows components of predicted gamma energy resolution that are due to electron energy resolution and to non-proportionality. These components are added in quadrature [see eqn. (5)] to obtain a prediction of gamma energy resolution. Electron energy resolution dominates at lower energy, while non-proportionality begins to additionally degrade gamma energy resolution above 60 keV. Fig. 12 shows that degradation due to non-proportionality does not vary dramatically as a function of the value of the extrapolated low-energy light output.

IV. Conclusion

There is reasonable agreement between gamma ray energy resolution measurements obtained by exciting NaI(Tl) with isotopic sources and values predicted from SLYNCI measurements of electron response and energy resolution and models for photon transport and electron cascade mechanisms. Low-energy extrapolation of the measured electron energy resolution has a larger effect on predicted gamma ray energy resolution than does low-energy extrapolation of measured electron light output. Gamma ray energy resolution is dominated by electron energy resolution at lower energy. Electron response non-proportionality additionally degrades gamma energy resolution above 60 keV.

Future directions include the use of GEANT4 to simulate the full cascade of energetic electrons emitted following photoelectric absorption of gamma rays, which will facilitate the study of non-proportionality and energy resolution for a variety of new scintillator materials.

Acknowledgment

This work was supported by the National Nuclear Security Administration, Office of Defense Nuclear Nonproliferation, Office of Nonproliferation Research and Development (NA-22) of the U. S. Department of Energy under Contract No. DE-AC03-76SF00098.

This document was prepared as an account of work sponsored by the United States Government. While this document is believed to contain correct information, neither the United States Government nor any agency thereof, nor The Regents of the University of California, nor any of their employees, makes any warranty, express or implied, or assumes any legal responsibility for the accuracy, completeness, or usefulness of any information, apparatus, product, or process disclosed, or represents that its use would not infringe privately owned rights. Reference herein to any specific commercial product, process, or service by its trade name, trademark, manufacturer,

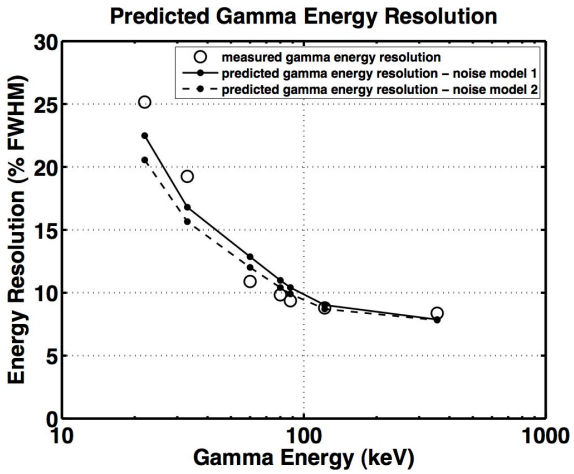

Fig. 10. Solid and dashed lines show gamma ray energy resolution predicted by noise models 1 and 2, respectively. Measured electron relative light output is extrapolated to 0.9 at low energy. Circles depict measured gamma ray energy resolution obtained with isotopic sources.

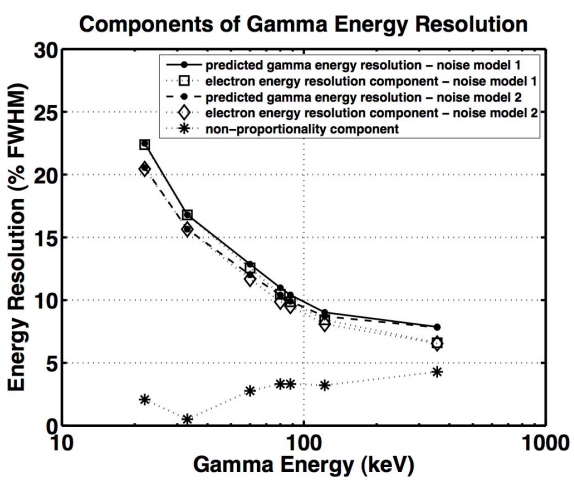

Fig. 11. Components of predicted gamma ray energy resolution shown in Fig. 10. Squares and diamonds depict electron energy resolution component [see eqn. (6)] predicted by noise models 1 and 2, respectively. Stars depict non-proportionality component [see eqn. (7)] predicted from measured electron relative light output that is extrapolated to 0.9 at low energy.

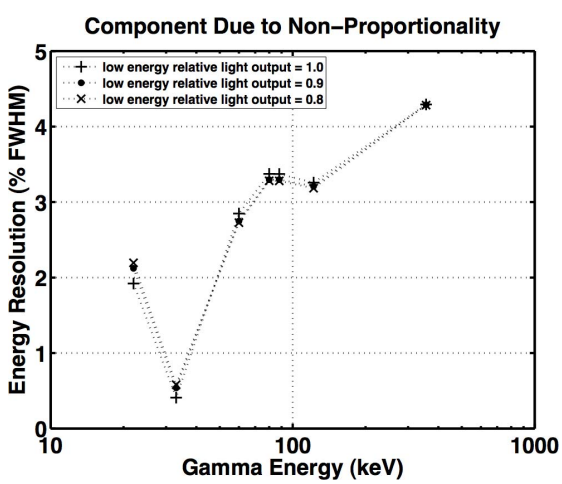

Fig. 12. Non-proportionality component of gamma ray energy resolution [see eqn. (7)] predicted from measured electron relative light output that is extrapolated to values of 1.0, 0.9, and 0.8 at low energy.

or otherwise, does not necessarily constitute or imply its endorsement, recommendation, or favoring by the United States Government or any agency thereof, or The Regents of the University of California. The views and opinions of authors expressed herein do not necessarily state or reflect those of the United States Government or any agency thereof or The Regents of the University of California.

REFERENCES

[1] C. D. Zerby, A. Meyer, and R. B. Murray, "Intrinsic line broadening in NaI(Tl) gamma-ray spectrometers," *Nucl. Instr. Meth.*, vol. 12, pp. 115–123, 1961.

[2] P. Dorenbos, J. T. M. de Haas, and C. W. E. van Eijk, "Non-proportionality in the scintillation response and the energy resolution obtainable with scintillation crystals," *IEEE Trans. Nucl. Sci.*, vol. 42, no. 6, pp. 2190–2202, 1995.

[3] W.-S. Choong, K. M. Vetter, W. W. Moses, G. Hull, S. A. Payne, N. J. Cherepy, and J. D. Valentine, "Design of a facility for measuring scintillator non-proportionality," *IEEE Trans. Nucl. Sci.*, accepted.

[4] B. D. Rooney and J. D. Valentine, "Scintillator light yield nonproportionality: Calculating photon response using measured electron response," *IEEE Trans. Nucl. Sci.*, vol. 44, no. 3, pp. 509–515, 1997.

[5] J. D. Valentine, B. D. Rooney, and J. Li, "The light yield nonproportionality component of scintillator energy resolution," *IEEE Trans. Nucl. Sci.*, vol. 45, no. 3, pp. 512–517, 1998.

[6] B. D. Rooney and J. D. Valentine, "Benchmarking the Compton coincidence technique for measuring electron response non-proportionality in inorganic scintillators," *IEEE Trans. Nucl. Sci.*, vol. 43, no. 3, pp. 1271–1276, 1996.

[7] S. Agostinelli, J. Allison, K. Amako *et al.*, "GEANT4 — a simulation toolkit," *Nucl. Instr. Meth.*, vol. A-506, no. 3, pp. 250–303, 2003.

[8] P. Billingsley, *Probability and Measure*, 3rd ed. New York, NY: John Wiley & Sons, 1995.